Chinese Chemical Letters 33 (2022) 4828–4833

Contents lists available at ScienceDirect

Chinese Chemical Letters

journal homepage: www.elsevier.com/locate/cclet

Effective norfloxacin elimination *via* photo-Fenton process over the MIL-101(Fe)-NH_2 immobilized on α-Al_2O_3 sheet

Qian Zhao, Chong-Chen Wang*, Peng Wang

Beijing Key Laboratory of Functional Materials for Building Structure and Environment Remediation/Beijing Energy Conservation & Sustainable Urban and Rural Development Provincial and Ministry Co-construction Collaboration Innovation Center, School of Environment and Energy Engineering, Beijing University of Civil Engineering and Architecture, Beijing 100044, China

ARTICLE INFO

Article history:
Received 22 November 2021
Revised 15 December 2021
Accepted 13 January 2022
Available online 16 January 2022

Keywords:
MIL-101(Fe)-NH_2@Al_2O_3 (MA)
Photo-Fenton
NOR
Mechanism
Real solar

ABSTRACT

MIL-101(Fe)-NH_2@Al_2O_3 (MA) catalysts were successfully synthesized by reactive seeding (RS) method on α-Al_2O_3 substrate, which demonstrated excellent photo-Fenton degradation performance toward fluoroquinolone antibiotics (*i.e.*, norfloxacin, ciprofloxacin, and enrofloxacin). The structure and morphology of the obtained MA were characterized by transmission electron microscopy (TEM), high-resolution transmission electron microscopy (HRTEM), atomic force microscope (AFM). The as-prepared MA could accomplish > 90% of norfloxacin degradation efficiency for 10 cycles' photo-Fenton processes, owing to its excellent chemical and water stability. In addition, the effects of operational factors including H_2O_2 concentration, foreign ions, and pH on the photo-Fenton degradation of norfloxacin over MA were clarified. The ESR spectra further document that $^{\bullet}O_2^-$, $^1O_2$ and $^{\bullet}OH$ radicals are prominent in the decomposition process of antibiotic molecules. Finally, the plausible photo-Fenton norfloxacin degradation mechanisms were proposed and verified.

Quinolone norfloxacin (NOR), a fluoroquinolone antibiotic, is widely used in both disease therapy and epidemic prevention of human being and animals [1]. It is found that NOR could be detected with relatively high concentrations (ng/L to several μg/L) in different wastewater and even surface water [2]. Its continuous input and bioaccumulation may trigger some serious problems like the induction of antibiotic-resistant bacteria and antibiotic resistance genes, which further exert a serious threat to creatures [3,4]. Therefore, the elimination of norfloxacin has become a pressing issue of public interest.

Up to now, various treatment methods including adsorption, electrochemical oxidation, advanced oxidation processes (AOPs) [5,6] have been reported to remove NOR, in which the advanced oxidation processes (AOPs) like Fenton reaction [7], photocatalysis, peroxymonosulfate activation, ozonation oxidation and their combination were affirmed to be effective for NOR removal [8]. Among the various AOPs, Fenton process utilizing ferrous ions (Fe^{2+}) to catalyze H_2O_2 to produce strong oxidizing $^{\bullet}OH$ was the widely used (Eqs. 1 and 2), which could destroy and mineralize toxic organic compounds in pharmaceutical effluents. The reaction rate illustrated in Eq. 1 is several orders of magnitude higher than that of Eq. 2 [9], resulting in a rapid consumption of iron ions (Fe(II)) and an excessive accumulation of iron ions (Fe(III)).

$$Fe^{2+} + H_2O_2 \rightarrow Fe^{3+} + {}^{\bullet}OH + OH^- \quad (K_1 \approx 70\,L\ mol^{-1}\ s^{-1}) \tag{1}$$

$$Fe^{3+} + H_2O_2 \rightarrow Fe^{2+} + {}^{\bullet}HO_2 + H^+ \quad (K_2 = 0.001\text{–}0.01\,L\ \ mol^{-1}\ \ s^{-1}) \tag{2}$$

Unfortunately, some inherent weaknesses like difficult separation and recyclability of the particle catalysts prevented the practical application of conventional homogeneous Fenton processes with an industrial scale [10]. Accordingly, it is highly desirable to seek the supported or immobilized catalysts with outstanding performances.

Metal-organic frameworks (MOFs) are a new type of three-dimensional porous materials consisting of metal clusters or ions as inorganic blocks linked by various organic linkers [11,12]. MOFs are promising in the fields of adsorption/separation, sensing, and catalysis, phototherapy, and drug delivery [8]. Noticeably, Fe-MOFs composed of oxygen-containing organic ligands and iron ions exhibit intrinsic visible light response properties due to the presence of Fe-O clusters [13,14], in which MIL-101(Fe)-NH_2 was assumed as a potential photo-Fenton catalyst as a result of their exceptional visible light harvesting capability and the highly dispersed

* Corresponding author.
E-mail address: chongchenwang@126.com (C.-C. Wang).

https://doi.org/10.1016/j.cclet.2022.01.033
1001-8417/

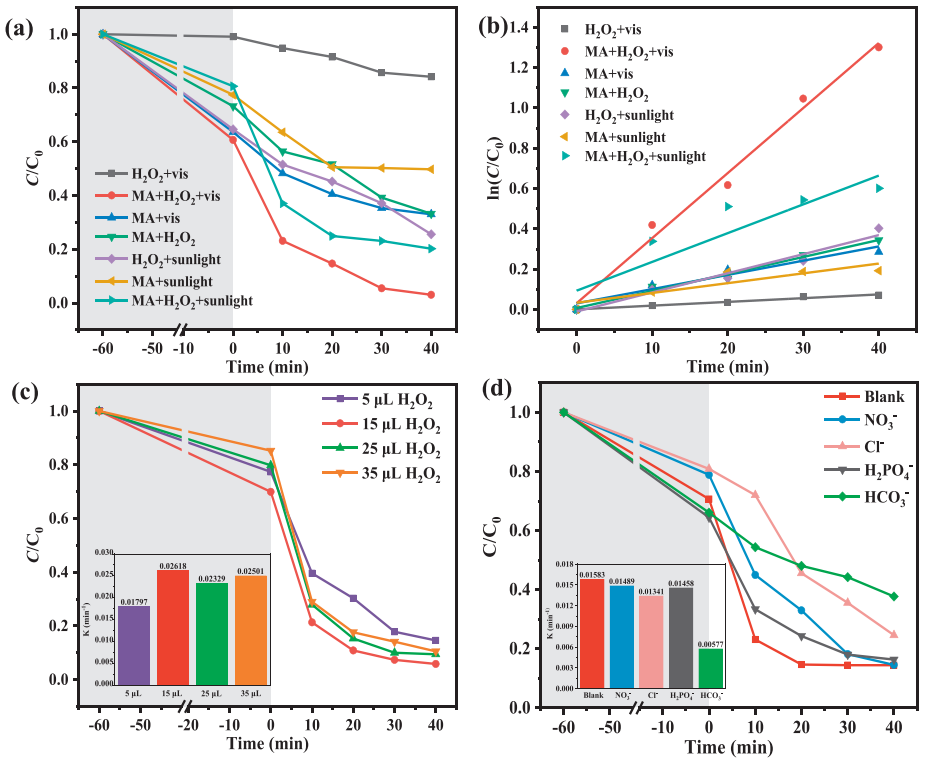

Fig. 1. (a) Catalytic NOR degradation efficiencies and (b) the reaction rates (k) of different systems. Influences of (c) H_2O_2 dosage, (d) foreign ions on the NOR degradation over MA.

Fe(II)/Fe(III) active sites [15,16]. As well, the powder MIL-101(Fe)-NH_2 catalyst proposed the challenges in scale-up process associated with the post-reaction particles recovery. For this reason, the immobilized catalysts on the substrate are more attractive than the powder catalysts, due to their facile scale-up and their easy recovery [17–19].

In our previous work, the effective photocatalytic Cr(VI) sequestration was achieved over the UiO-66(Zr/Hf)-NH_2 membrane [20] and the MIL-101(Fe)-NH_2 immobilized on alumina substrate [21]. Following our previous work, the MIL-101(Fe)-NH_2@Al_2O_3 (MA) was hydrothermally synthesized by a reactive seeding method. The characterizations of the as-prepared MA were provided in the Supplementary material, which matched well with our previous work [21].

The photo-Fenton catalytic activity of the prepared MA was evaluated in a jacket-glass reactor under a 300 W Xe lamp (Beijing Aulight Co., Ltd.) irradiation (Fig. S5 in Supporting information) adopting a typical fluoroquinolone antibiotic NOR as model pollutant. Firstly, a piece of MA (the actual immobilized MIL-101(Fe)-NH_2 being *ca.* 15 mg) was spiked into 50.0 mL NOR aqueous solution (10 mg/L) with continuous stirring for 60 min to reach the adsorption-desorption equilibrium before the visible light irradiation and the addition of 15 μL 30% H_2O_2 solution. At the pre-determined intervals (10 min), 1.5 mL of filtrate was collected, in which 10 μL isopropanol was added to remove the residual H_2O_2. The concentration of residual NOR was measured by ultra-high performance liquid chromatography (UHPLC, Thermo Scientific Vanquish Flex).

The NOR removal efficiencies and degradation kinetics in different systems were displayed in Figs. 1a and b. Under the dark condition, the uptakes of NOR of MA can reach saturation within 60 min, in which about 40.0% of NOR was adsorbed. The MIL-101(Fe)-NH_2 could act as visible responsive photocatalyst to accomplish organics decomposition [22]. In the presence of H_2O_2, the individual MIL-101(Fe)-NH_2 can undergo heterogeneous photo-Fenton reaction to enhance the organic pollutants degradation efficiency [23]. Due to the synergistic effect of photocatalysis and heterogeneous Fenton reaction, 97.3% NOR can be effective degraded in the MA/H_2O_2/vis system within 100 min (Fig. 1a). Upon the irradiation of visible light, MIL-101(Fe)-NH_2 could generate h^+ and e^- following Eq. 3. The introduced H_2O_2 could trap e^- to form $^{\bullet}OH$ radicals, which inhibited the recombination of h^+ and e^- and further improved the NOR degradation (Eq. 4). In the H_2O_2/vis system, *ca.* 15% NOR was decomposed after 100 min, which might be assigned to the major oxidation of holes or auxiliary oxidative degradation by $^{\bullet}OH$ and $^{\bullet}O_2^-$ [24,25]. In the MA/H_2O_2 system, the NOR degradation efficiency increased noticeably, due to that the Fe-O clusters of MIL-101(Fe)-NH_2 on the surface of the MA can activate H_2O_2 to produce more $^{\bullet}OH$ radicals (Eqs. 5 and 6). In the MA/vis condition, *ca.* 40% NOR removal was achieved, in which the formed $^{\bullet}O_2^-$ radicals produced on the HOMO of MIL-101(Fe)-NH_2 can be transferred into $^{\bullet}OH$ following the multi-step free radical reaction processes (Eqs. 7 and 8).

The *pseudo*-first order kinetic could be introduced to determine the NOR degradation rates of different reaction systems (Fig. 1b). The results revealed that the calculated k of the NOR degradation in the MA/H_2O_2/vis system was 3.23×10^{-2} min^{-1}, which was *ca.* 17.0, 3.8, 4.6 and 2.2 times higher than those in the H_2O_2/vis (1.9×10^{-3} min^{-1}), MA/H_2O_2 (8.5×10^{-3} min^{-1}), MA/vis (7.0×10^{-3} min^{-1}) and MA/H_2O_2/sunlight (14.3×10^{-3} min^{-1}) systems, respectively.

$$MA + h\nu \rightarrow MA\ (h^+ + e^-) \quad (3)$$

$$H_2O_2 + e^- \rightarrow {}^{\bullet}OH + HO^- \quad (4)$$

$$Fe(III) + H_2O_2 \rightarrow Fe(II) + {}^{\bullet}HOO/{}^{\bullet}O_2^- + H^+ \quad (5)$$

$$Fe(II) + H_2O_2 \rightarrow Fe(III) + {}^{\bullet}OH + OH^- \quad (6)$$

$$\bullet O_2^- + H_2O \rightarrow {}^{\bullet}OOH + OH^- \quad (7)$$

$$\bullet OOH + H_2O + 2e^- \rightarrow {}^{\bullet}OH + 2OH^- \quad (8)$$

To elucidate the effect of H_2O_2 dosage on the NOR degradation, some experiments (Fig. 1c) based on different dosages of H_2O_2 (5, 15, 25 and 35 μL) were conducted. As the H_2O_2/NOR molar ratio increased from 31:1 to 93:1, the NOR degradation rate constants increased from 0.01797 min^{-1} to 0.02618 min^{-1} due to the increasing ·OH radicals [25]. When the H_2O_2/NOR molar ratio was over 93:1, the NOR removal rates decreased slightly, due to that the excessive H_2O_2 might scavenge ·OH radicals (Eqs. 9 and 10) [26]. Finally, 15 μL H_2O_2 was adopted as the optimum dosage for the NOR decomposition.

$$H_2O_2 + {}^{\bullet}OH \rightarrow {}^{\bullet}HO_2 + H_2O \quad (9)$$

$$\bullet HO_2 + {}^{\bullet}OH \rightarrow H_2O + O_2 \quad (10)$$

Various inorganic anions are commonly found in aqueous media, which might significantly affect the organic pollutants degradation in the advanced oxidation processes [27]. The influences of the different anions were clarified by adding 20 mmol/L corresponding anions to the MA/H_2O_2/vis system (Fig. 1d). All the selected inorganic anions inhibited the NOR degradation efficiencies in varying degrees, leading to the *k* values followed the order of no anions (0.01583 min^{-1}) > NO_3^- (0.01489 min^{-1}) > $H_2PO_4^-$ (0.01458 min^{-1}) > Cl^- (0.01341 min^{-1}) > HCO_3^- (0.00577 min^{-1}). It was obvious that the HCO_3^- and Cl^- displayed significant inhibitory effects on NOR degradation. HCO_3^- could greatly inhibit NOR degradation due to that HCO_3^- and CO_3^{2-} competed with hydroxyl (·OH) to yield weak oxidants ($CO_3^{-\bullet}$ and $HCO_3^{\bullet}$) (Eqs. 11-13). Generally, the Cl^- and NO_3^- can react with ·OH radicals to yield less-reactive radicals like $Cl^{\bullet}$ and $NO_3^{\bullet}$ (Eqs. 14 and 15). It was reported that $H_2PO_4^-$ could act as a chelating agent to block the surface Fe sites of Fe-MOFs [28], resulting in a quenching effect for radicals.

$$\bullet OH + HCO_3^- \rightarrow CO_3^{-\bullet} + H_2O \quad (11)$$

$$HCO_3^- \rightarrow H^+ + CO_3^{2-} \quad (12)$$

$$CO_3^{2-} + {}^{\bullet}OH \rightarrow OH^- + CO_3^{-\bullet} \quad (13)$$

$$Cl^- + {}^{\bullet}OH \rightarrow Cl^{\bullet} + OH^- \quad (14)$$

$$NO_3^- + {}^{\bullet}OH \rightarrow NO_3^{\bullet} + OH^- \quad (15)$$

The influence of different pH values ranging from 2.95 to 11.0 on the NOR degradation efficiencies was also investigated. As shown in Fig. S7a (Supporting information), 80.0%∼97.3% NOR can be degraded within 50 min at a wide pH range from 2.95 to 11.0, verifying the effective NOR decomposition in the MA/H_2O_2/vis system could be achieved over a wide pH range.

As well, pH might exert an effect on the molecular form and surface charge of norfloxacin. Intense adsorption occurred in pH range of 5.5–6.34 with the maximum adsorption at pH 5.5 (Fig. S7a), due to the dissociation constants of norfloxacin (p*K*a 6.34 and 8.75) [29]. The weaker adsorption at extremely low (pH 2.95) and high (pH 11.0) pH conditions can be attributed to the strong electrostatic repulsive force between NOR and the MIL-101(Fe)-NH_2 in MA, as both NOR and MA were mainly positively charged at low pH (<3.26) and negatively charged at high pH (>8.75) [30].

To clarify the reaction mechanism of the MA/H_2O_2/vis system, the trapping experiments were carried out to identify the contribution of hydroxyl radicals (·OH), holes (h^+), superoxide radical anions ($^{\bullet}O_2^-$) and singlet oxygen ($^1O_2$) in the NOR degradation process (Fig. S8a in Supporting information). As shown in Fig. 2a, the NOR degradation efficiency decreased by 14.3%, 8.8% and 4.7% after adding *tert*–butyl alcohol (TBA), L-histidine and benzoquinone (BQ), respectively. It implied that ·OH, $^1O_2$, and $^{\bullet}O_2^-$ contributed to the photo-Fenton reaction, in which ·OH radicals play more significant role in this process.

Furthermore, ESR measurements proved the existence of $^{\bullet}O_2^-$, $^1O_2$ and ·OH, affirming the result of active species trapping experiments. As shown in Figs. 2b and c, the DMPO-$^1O_2$ and DMPO-$^{\bullet}O_2^-$ signals were observed upon the visible light irradiation for 5 min and 10 min, while no corresponding signals were detected in dark condition, confirming the generation of $^1O_2$ and $^{\bullet}O_2^-$ during both photocatalysis process and photo-Fenton processes. As shown in Fig. 2d, DMPO-·OH signals were observed in MA/H_2O_2/dark system, implying that ·OH radical generated through Eqs. 5 and 6 played primary roles in the NOR degradation.

As reported previously [31], terephthalic acid can selectively react with ·OH radicals to form 2–hydroxy terephthalic acid which can emit fluoresce at 425 nm when excited at 315 nm. It was observed that the intensity of the PL peak increased greatly in MA/H_2O_2/vis system, suggesting the increasing formation of ·OH radicals. It corresponded well with the results illustrated in Fig. S9a (Supporting information) and the results of ESR (Figs. 2b-d), further confirming the important role of ·OH radical in the degradation process. Increasing ·OH radicals can be generated in the MA/H_2O_2/vis system, in which the fluorescence intensity increased with the reaction time (Fig. S8b in Supporting information). Furthermore, the quantitative determination of the ·OH generated from MA/H_2O_2/vis system was conducted, in which 477.3 μmol/L of ·OH radicals can be yielded within 80.0 min (Fig. S9b in Supporting information)

In the mechanism illustration (Fig. 3a), it can be found that ·OH can be generated through two pathways: (i) The Fenton-like reaction was the pre-dominant one (Fig. 1a); (ii) the photocatalysis contributed a minor part. H_2O_2 will capture the photogenerated electrons from MIL-101(Fe)-NH_2 in MA to produce ·OH, thereby inhibiting the electron-hole recombination and enhancing the degradation efficiency of pollutants (Eqs. 3 and 4).

Partial $^{\bullet}O_2^-$ radicals were produced by the reduction reaction of oxygen and electron under the oxygen-rich condition (Eq. 16). Subsequently, the $^{\bullet}O_2^-$ radicals were immediately converted to $^1O_2$ by the oxidation of holes (Eq. 17) [32]. The formation of $^{\bullet}O_2^-$ radicals in large quantities promoted the redox reaction with Fe(III), and further facilitated the generation of ·OH radicals (Eq. 18).

$$O_2 + e^- \rightarrow {}^{\bullet}O_2^- \quad (16)$$

$$\bullet O_2^- + h^+ \rightarrow {}^1O_2 \quad (17)$$

$$Fe(III) + {}^{\bullet}O_2^- \rightarrow Fe(II) + O_2 \quad (18)$$

According to the theoretical calculation of the main active sites of norfloxacin by Bao *et al*. [33], the higher Fukui indexes (f^0) of C2,

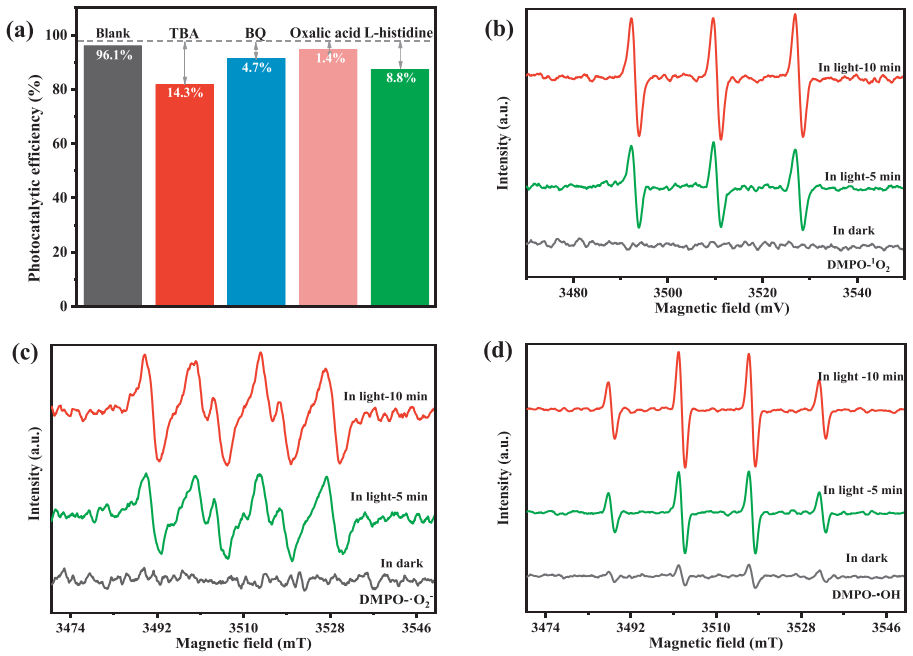

Fig. 2. (a) Reactive species trapping experiments for NOR degradation over MA. The ESR spectra of (b) DMPO-$^1O_2$, (c) DMPO-$\cdot O_2^-$ and (d) DMPO-•OH.

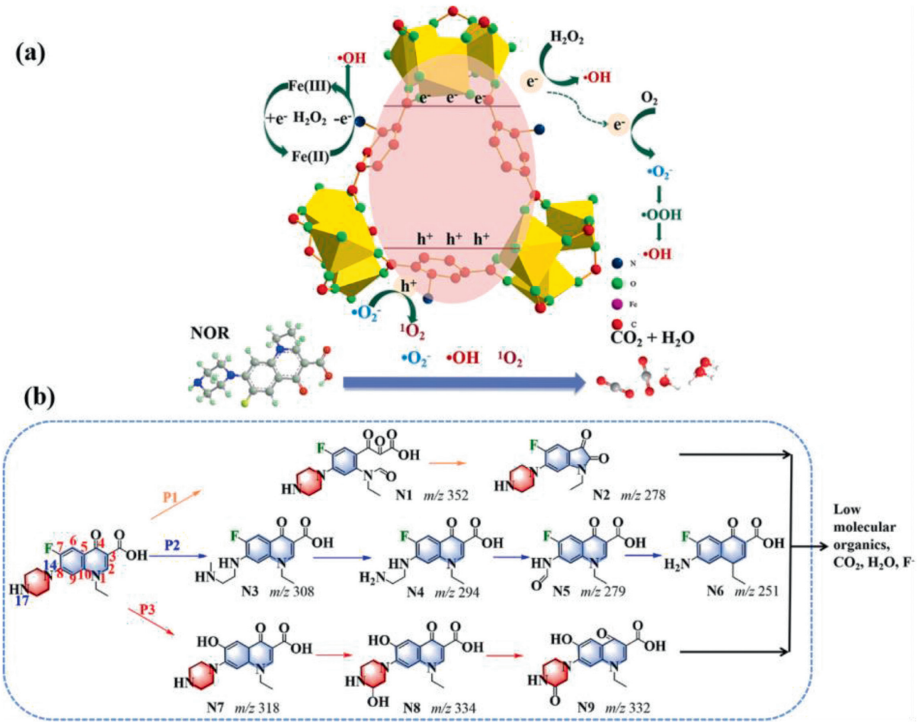

Fig. 3. (a) The proposed photocatalytic mechanism of MA/H_2O_2/vis system to degrade NOR. (b) Degradation pathways of NOR in MA/H_2O_2/vis system.

C3, C4, N14 and N17 in the NOR molecule are the major active sites for radical attack. The highest occupied molecular orbital (HOMO) of NOR was mainly distributed in the marginal parts of the piperazine ring and quinolone, indicating that these regions are susceptible to electron loss and attack by •OH. It was previously reported that the piperazine ring was positive region of the NOR molecule, further confirming that the piperazine ring was more easy to be attacked by the •OH radicals [34].

The formed intermediates during the NOR decomposition in the MA/H_2O_2/vis system were further tested by HPLC-ESI-MS. Nine different organic intermediates were identified with *m/z* 304, *m/z* 276, *m/z* 308, *m/z* 294, *m/z* 279, *m/z* 269, *m/z* 318, *m/z* 334, *m/z* 332, respectively. The molecular weights of the intermediates and proposed molecular structure are summarized in Table S2 (Supporting information).

Combining experimental analyses and theoretical calculation, the possible NOR degradation pathways were proposed (Fig. 3b). The pathways of NOR degradation were classified as quinolone group transformation (P1) [35], and oxidation of the piperazine ring (P2) [29], defluorination (P3) [36].

In the pathway 1 (quinolone group transformation), the C=C bond of the quinolone group was attacked and broken by •OH,

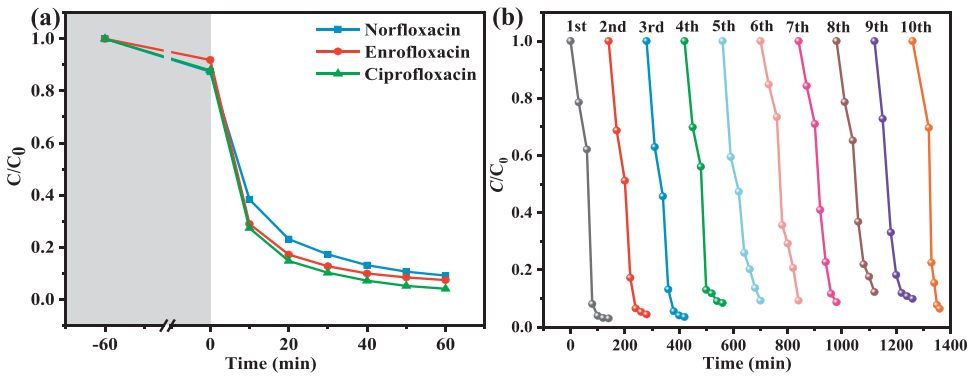

Fig. 4. (a) Performance comparison of MA degradation of quinolone antibiotics. (b) Reusability test of NOR degradation over MA under visible light irradiation.

in which **N1** was formed, and then **N2** was formed by decarboxylation. Pathway 2 mainly described the ring-opening reaction of the piperazine ring. The NOR would be split through oxidative re-arrangements of the piperazine ring [37,38], to form **N3**, **N4**, **N5**, **N6**. With the further oxidation of $^{\bullet}OH$, $^{\bullet}O_2^-$ and $^1O_2$, the piperazine ring was opened and the -C_2H_2- group was dropped to yield the intermittent product **N4** [39]. Subsequently, the CH_3N was lost from the -NH–CH_2-CH_2-NH_2 group in **N4** to produce **N5** (*m/z* 279), as well as decarbonylated to amine -NH_2 (N6). In pathway P3, the F atom could also be attacked by $^{\bullet}OH$ and substituted by hydroxyl groups, forming **N7** (*m/z* 318). After hydroxylation and dehydrogenation, it would be further converted to **N8** (*m/z* 334) and **N9** (*m/z* 332) [40]. In all, the above-mentioned intermediates would be further oxidized by different active species to low molecular weight organic and inorganic products, *e.g.*, CO_2 and H_2O.

Furthermore, MA also demonstrated good performance in degrading different quinolone antibiotics (Fig. 4a). The degradation efficiencies toward other organic contaminants such as norfloxacin (NOR), ciprofloxacin (CIP), and enrofloxacin (ENR) in MA/H_2O_2/vis system were also evaluated, in which 90.9% of NOR, 95.9% of CIP, and 92.6% of ENR could be removed within 120 min, indicating that MA demonstrated high degradation ability for various quinolone antibiotics.

It is widely acknowledged that the stability and reusability of photocatalysts are very essential from an economic aspect. As shown in Fig. 4b, the recycling test showed that the catalysis activity maintained well during the recycling, in which 97.0% NOR removal efficiency can still be achieved even after recycling for 10 times (totally 1400 min). Obviously, the XPS spectra (Fig. S10 in Supporting information) of used MA matched well with original samples, further confirming its stability. It can be concluded that MA exhibited outstanding photo-Fenton performance and reusability, which was superior to most counterpart catalysts (Table S3 in Supporting information).

During NOR degradation, it was essential to consider the toxicity of the degradation intermediates. The acute toxicity (Fathead minnow), bioaccumulation factors of NOR and its degradation intermediates were assessed by using Toxicity Estimation Software Tool (T.E.S.T.) based on quantitative structure-activity relationship (QSAR) model [41]. As shown in Fig. S11a (Supporting information), the LC_{50} of fathead minnow was 2.24 mg/L for NOR, which can be categorized as "Toxic". The three degradation products, **N4**, **N7** and **N9** displayed high LC_{50} values. And, the toxicity of all other degradation products decreased, compared to that of the pristine NOR. Fig. S11b (Supporting information) revealed that the MA/H_2O_2/vis systems can decrease the bioaccumulation factor of most of the intermediates except product **N2** and **N3**. The combined results displayed that the MA/H_2O_2/vis systems could degrade NOR into some intermediates with lower toxicity or even into some inorganic molecules.

In all, the as-synthesized MA exhibited the efficiency of NOR degradation under the visible light and real solar light, in which more than 90% of NOR was mineralized in the presence of H_2O_2. Three possible pathways for catalytic photo-Fenton NOR degradation were proposed based on the HPLC/MS analyses and Fukui indexes. It was worth noting that MIL-101(Fe)-NH_2@Al_2O_3 (MA) catalysts can overcome the disadvantage that the conventional powder MOFs were difficult to be recycled and reused. The as-prepared MA maintained excellent removal efficiencies over a wide range of pH values and long-term operations. Without the requirement of separating the MA from the reaction solution, the fabricated MA demonstrated great potential for practical wastewater treatment.

Declaration of competing interest

The authors declare that they have no known competing financial interests or personal relationships that could have appeared to influence the work reported in this paper.

Acknowledgments

This work was supported by National Natural Science Foundation of China (No. 22176012), Beijing Natural Science Foundation (No. 8202016).

Supplementary materials

Supplementary material associated with this article can be found, in the online version, at doi:10.1016/j.cclet.2022.01.033.

References

[1] Y. Picó, V. Andreu, Anal. Bioanal. Chem. Res. 387 (2007) 1287–1299.
[2] Y. Chen, T. Lan, L. Duan, et al., PLoS One 10 (2015) e0145025.
[3] M. Li, D. Wei, H. Zhao, et al., Chemosphere 95 (2014) 220–226.
[4] Q. Zeng, S. Chang, M. Wang, et al., Chin. Chem. Lett. 32 (2021) 2212–2216.
[5] J. Rivas, A. Encinas, F. Beltran, et al., J. Environ. Sci. Health A 46 (2011) 944–951.
[6] F. Li, Z. Wei, K. He, et al., Water Res. 185 (2020) 116219.
[7] Y. Pi, J. Feng, M. Song, et al., Chin. Sci. Bull. 59 (2014) 2618–2624.
[8] J.J. Pignatello, E. Oliveros, A. MacKay, Crit. Rev. Environ. Sci. Technol. 36 (2006) 1–84.
[9] B. Ponnusami, K. Muthukumar, J. Environ. Chem. Eng. 2 (2014) 557–572.
[10] D. Wang, D. Astruc, Chem. Rev. 114 (2014) 6949–6985.
[11] D. Ma, S. Peh, H. Gang, et al., ACS Appl. Mater. Interfaces 9 (2017) 7523–7534.
[12] H. Fu, C.C. Wang, W. Liu, Chin. Chem. Lett. 33 (2022) 1647–1649.
[13] X.H. Yi, C.C. Wang, Prog. Chem. 3 (2021) 471–489.
[14] J. Huang, K. Li, L. Wang, et al., Chin. Chem. Lett. 33 (2022) 3787–3791.
[15] D. Wang, R. Huang, W. Liu, et al., ACS Catal. 4 (2014) 4254–4260.
[16] Q. Wu, H. Yang, L. Kang, et al., Appl. Catal. B 263 (2020) 118282.
[17] J. Maina, J. Schütz, L. Grundy, et al., ACS Appl. Mater. Interfaces 9 (2017) 35010–35017.
[18] R. Molinari, T. Marino, A. Pietro, Int. J. Hydrogen Energy 39 (2014) 7247–7261.

[19] Y. Liu, F. Liu, N. Ding, et al., Chin. Chem. Lett. 31 (2020) 2539–2548.
[20] X.D. Du, X.H. Yi, P. Wang, et al., Chem. Eng. J. 356 (2019) 393–399.
[21] Q. Zhao, X.H. Yi, C.C. Wang, et al., Chem. Eng. J. 429 (2022) 132497.
[22] Z. Zhang, X. Li, B. Liu, et al., RSC Adv. 6 (2015) 4289.
[23] M. Cheng, C. Lai, Y. Liu, et al., Coord. Chem. Rev. 368 (2018) 80–92.
[24] H. Fu, X.X. Song, L. Wu, et al., Mater. Res. Bull. 125 (2020) 110806.
[25] M. Xia, M. Long, Y. Yang, et al., Appl. Catal. B 110 (2011) 118–125.
[26] Q. Chen, P. Wu, Y. Li, et al., J. Hazard. Mater. 168 (2009) 901–908.
[27] X.H. Yi, H. Ji, C.C. Wang, et al., Appl. Catal. B 293 (2021) 120229.
[28] F.X. Wang, C.C. Wang, X. Du, et al., Chem. Eng. J. 429 (2022) 132495.
[29] X. Chen, R. Zhuan, J. Wang, et al., J. Hazard. Mater. 404 (2021) 124172.
[30] W. Liu, J. Zhang, C. Zhang, et al., Chem. Eng. J. 171 (2011) 431–438.
[31] V. Sharma, M. Feng, J. Hazard. Mater. 372 (2017) 3–16.
[32] J.M. Monteagudo, A. Durán, M.R. Martínez, et al., Chem. Eng. J. 380 (2020) 122410.
[33] C.S. Bao, J. Zhao, Y.Y. Sun, et al., Environ. Sci. Nano 8 (2021) 2347–2359.
[34] H. Li, J. Chen, H. Hou, et al., Water Res. 126 (2017) 274–284.
[35] C. Wang, G. Yu, H. Chen, et al., Chemosphere 270 (2021) 129408.
[36] H. Chen, J.L. Wang, J. Hazard. Mater. 403 (2020) 123697.
[37] M.J. Chen, W. Chu, Appl. Catal. B 168-169 (2015) 175–182.
[38] M. Huang, T. Zhou, X. Wu, et al., Water Res. 119 (2017) 47–56.
[39] D. Ding, C. Liu, Y. Ji, et al., Chem. Eng. J. 308 (2017) 330–339.
[40] D. Yu, J. He, Z. Wang, et al., Chem. Eng. J. 417 (2021) 129240.
[41] R. Yin, Y. Chen, S. He, et al., J. Hazard. Mater. 388 (2020) 121996.